

# IMPROVEMENT OF UNSTEADY AERODYNAMIC LOADS PREDICTION OF THE DOUBLET-LATTICE METHOD USING SMALL DISTURBANCE CFD

Cyrille Vidy<sup>1</sup>, Lukas Katzenmeier<sup>2</sup>

<sup>1</sup> Airbus Defence and Space, Structural Dynamics & Aeroelasticity TEAGD  
Rechliner Strasse, D-85077 Manching, Germany  
cyrille.vidy@airbus.com

<sup>2</sup> Airbus Defence and Space, Acoustics & Vibrations TEAGX  
Rechliner Strasse, D-85077 Manching, Germany  
lukas.katzenmeier@airbus.com

**Keywords:** Aeroelasticity, Structural Dynamics, Small-Disturbance CFD, DLM-correction.

**Abstract:** This paper shows a correction method for classical potential aerodynamic method such as the subsonic Doublet-Lattice Method (DLM) or the supersonic method ZONA51, both widely used for aeroelastic computations. This particular correction method is based on small disturbance CFD, a very robust and efficient tool to derive linearized aerodynamic forces for aeroelasticity with CFD quality. It is based on a multiplicative correction of the aerodynamic influence coefficients (AIC) and on additive correction terms. A first assessment of the improvements to the DLM generalized aerodynamic forces (GAFs) is done using the NLR7301 airfoil, then the effects of this correction technique for flutter analysis are presented using the flying wing configuration SACCON (DLR-F19) and compared with DLM and small disturbance CFD results.

## 1 INTRODUCTION

In the last decades, the use of CFD tools for the prediction of motion-induced or gust-induced aerodynamic loads has been tested with promising results. In the same time, several small disturbance CFD tools have been implemented, based on the linearization of the Euler or RANS equations in the frequency domain [1]. These tools have the ability to deliver generalized aerodynamic forces (GAFs) for linear aeroelastic analyses with good accuracy and less computational effort than nonlinear solutions [2].

However, the computational power needed to generate a full dataset is still high in comparison to the Doublet-Lattice Method (DLM) [3]. For this reason, an AIC-correction technique was implemented by Airbus Defence and Space in cooperation with the Technical University of Munich [4] [5]. It is based on the small-disturbance CFD tool AER-SDNS [1]. This legacy correction method has been improved and completed with further correction terms in order to correctly estimate motions and forces in flow-direction, as it is needed for T-tails [6] or configurations with in-plane flutter modes.

This paper shows the improved correction technique for DLM/ZONA51 using AER-SDNS inputs for the NLR7301 airfoil [7] and the SACCON flying wing configuration [8] [9].

## 2 CORRECTION METHOD

The AIC (downwash) correction technique developed by Airbus Defence and Space in cooperation with the Technical University of Munich has already shown promising results for flutter analysis [4, 5]. The new correction terms introduced in this paper are based on the steady reference state computed with AER-NS or on results of AER-SDNS for a specific flight-mechanic mode.

The first improvement is an adjustment of the force direction for each aerodynamic box of the DLM-model. The pressure forces of AER-SDNS are not necessarily normal to the chord-direction and induce some pressure forces in this chord-direction. These forces are not negligible when in-plane modes have to be considered. The AIC-correction now considers this change of normal vectors.

The second improvement is an estimate of the forces induced by a motion in the flow direction by assuming this motion to create a local change in dynamic pressure. This estimate works well for low reduced frequencies and for the lower eigenmodes of each lifting surface.

The last improvement bases on the perturbed surface vectors for specific modal motions that can lead to non-negligible terms in the GAF-matrices, as for the influence of other modes on in-plane modes.

In order to better understand the three improvements to the AIC-correction presented in the following, it is helpful to show the computation of the disturbance force normalized with the dynamic pressure at each force application point of the CFD surface:

$$\frac{\widehat{df}}{\widehat{q_\infty}} = - \left( \widehat{c_p} \overline{dS} + \overline{c_p} \widehat{dS} + \frac{\widehat{q_\infty}}{\overline{q_\infty}} \overline{c_p} \overline{dS} \right). \quad (1)$$

In equation 1, the accentuated terms are the first order perturbations calculated around the reference steady term (marked with bars). Since AER-SDNS results of this paper use Euler equations, friction terms are not included here. The last term is normally not included if one computes directly with AER-SDNS all the aerodynamic forces due to flight-mechanical motions.

The forces built with AICs from DLM/ZONA51 only consider the first term of equation 1. Even with AIC-correction, only this term can be expected from the AIC-part. However, even after having transformed the AER-SDNS forces with IPS-splines back to the DLM lifting points, these forces are not fully normal to the DLM boxes. For each box, the normal vectors are then realigned with the pressure disturbance forces of the pitching mode at reduced frequency 0. This effect is higher at the leading and trailing edges, and very low for the rest of the model.

The second part of the correction bases on the third term of equation 1. The first correction has namely taken into account a more three-dimensional orientation of the pressure forces, but can still not take into account motions in the flow direction. In order to estimate this effect, the disturbance in dynamic pressure is estimated out of the local disturbance in velocity of each collocation point of DLM as presented in equation 2.

$$\widehat{q_\infty} \approx -\rho_\infty U_\infty \left( \frac{jk}{L_{ref}} \right) \widehat{x} \quad (2)$$

In equation 2, the upstream density  $\rho_\infty$  and flow velocity  $U_\infty$  are used. The term with the reduced frequency  $k$  and the reference length  $L_{ref}$  represents the first derivative in the frequency domain of the disturbance of the position  $x$  of each force application point in flow direction. This computation can be done using the DLM mesh instead of the CFD mesh after having splined the steady aerodynamic pressures on the DLM boxes. The resulting GAFs are then added to the AIC-based GAFs. One can note that this term has only an effect on the imaginary part of the GAFs and is based on quasi-steady considerations.

The last part of the correction uses the second term of equation 1 where it can be seen that only the perturbation of the surface vectors has to be computed in the AER-SDNS mesh in order to take this effect into account. Thus, no additional CFD-effort is required. Also this term can be added to the DLM GAFs. This term is independent of the reduced frequency and has only an effect on the real part of the GAFs.

### 3 NLR7301 RESULTS

The first model used in this paper is the NLR7301 airfoil (Figure 1, [7]). It is asymmetric and has some rear loading and is therefore a quite realistic example of aerodynamics around an aircraft wing.

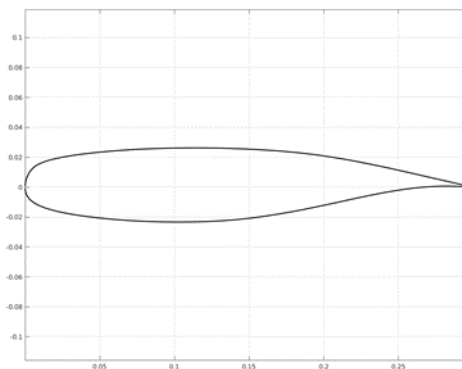


Figure 1: NLR7301 airfoil

The NLR7301 airfoil is known for transonic effects, however the Mach number considered in the following is Mach 0.4 in order to have a better comparison between DLM and AER-SDNS.

#### 3.1 Analysis description

The DLM model has 12 boxes equally spaced in the chord direction. The span of the model was chosen in order to obtain a high aspect ratio and to obtain quasi 2D conditions. The boxes with same chordwise position were moved together and the forces summed up at each chordwise position, thus obtaining a 2D DLM model with AICs dimension 12\*12.

The considered eigenmodes are rigid-body translation in the chord direction (mode 1), in the heave direction (mode 2) and in the pitch direction (mode 3). The rotation point of the pitching mode has been chosen at 40% of the chord, since the steady lift force application point of this profile lies near 50% of the chord for the chosen angle of attack of  $0.6^\circ$ .

The AIC-correction was trained using inputs from mode 2 (heave) and 3 (pitch).

### 3.2 Aerodynamic results

In Figure 2 and 3, different generalized aerodynamic forces are plotted along the reduced frequency as real part (full lines) and imaginary part (dashed lines). The blue lines represent the AER-SDNS results, the red ones the uncorrected DLM results, and the yellow ones the results of the present correction method. The GAF entries for other modes show similar behaviors.

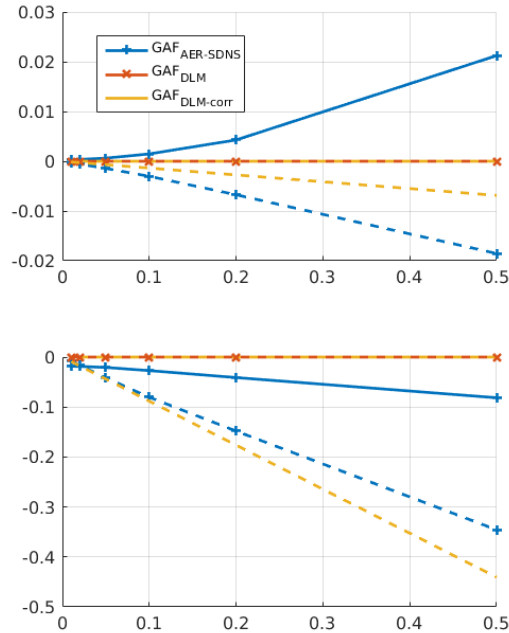


Figure 2: Aerodynamic forces induced by mode 1, generalized with mode 1 and 2

In Figure 2, the influence of the dynamic pressure correction becomes apparent. It acts only on the imaginary part of the GAF and matches well the CFD in the case of the influence of the mode 1 on mode 2, especially at low frequencies. The influence of mode 1 on itself is very low and the higher relative differences are expected to have less influence on the aeroelastic results.

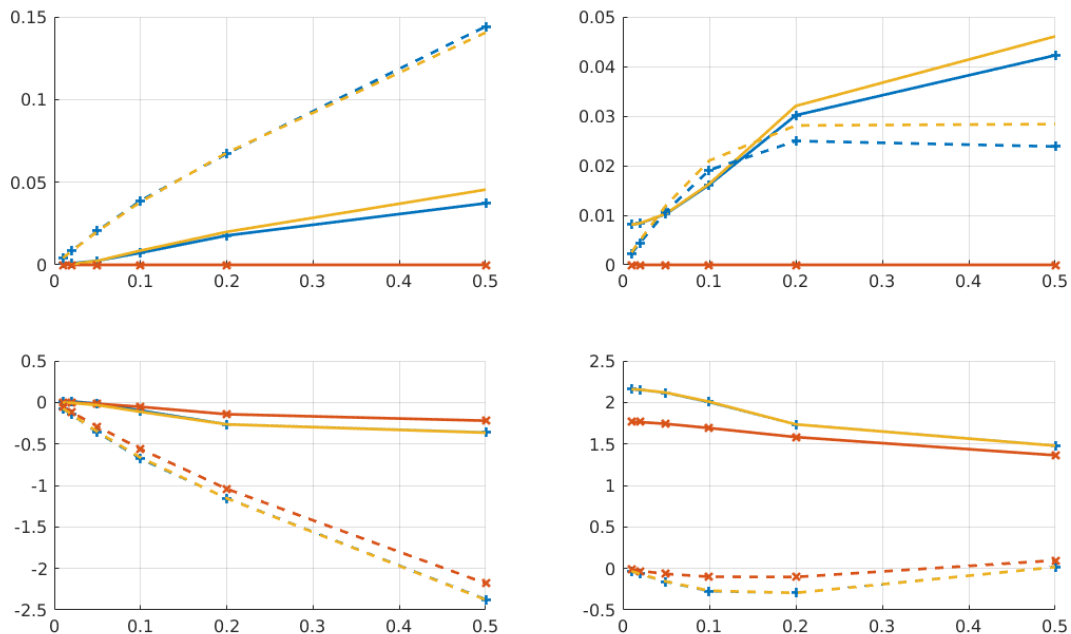


Figure 3: Aerodynamic forces induced by mode 2 and 3, generalized with mode 1 and 2

In Figure 3, all results of the correction present a very strong improvement of the GAF. This applies for the influence of mode 2 and 3 on mode 2, which is mostly a consequence of the legacy AIC-correction. This applies also for the influence of mode 2 and especially 3 on mode 1, where also the surface correction is needed in order to match correctly the AER-SDNS GAF. This can be seen when the different parts of the GAFs are plotted separately as in Figure 4.

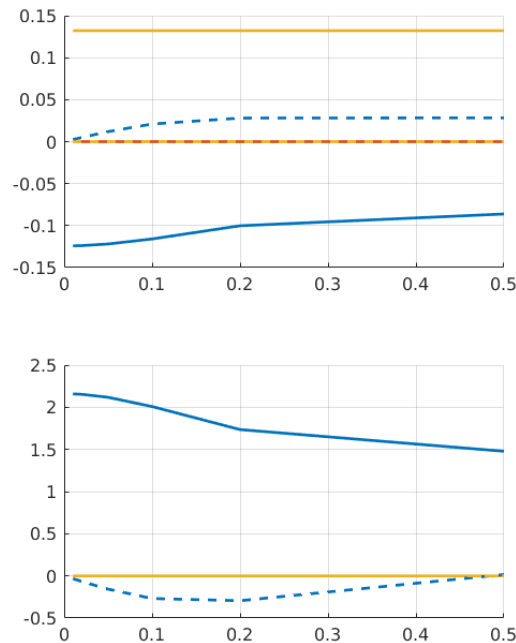


Figure 4: Aerodynamic forces induced by mode 3, generalized with mode 1 and 2

In Figure 4, the AIC corrected GAFs are plotted in blue (real parts as full lines, imaginary parts as dashed lines), the surface correction part of the GAFs in yellow and the dynamic pressure correction parts in red. Mode 3 is a pitch mode, thus no dynamic pressure correction applies. The effect of the corrected normals becomes very apparent in the AIC corrected GAFs from mode 3 on mode 1, as well as the influence of the surface correction. The sum of these corrected GAFs matches very well the AER-SDNS GAFs as already seen in Figure 3.

The presented results prove the potential of the present correction method for a simple model. In the following section, a more realistic airplane model is used in order to assess the aeroelastic prediction improvements based on this method.

## 4 SACCON RESULTS

The SACCON configuration (also known as DLR-F19) has been developed within the cooperation project Mephisto between the DLR and Airbus Defence and Space [8]. This flying wing configuration has been analyzed with several aerodynamic methods in order to assess flutter [9], including DLM, ZONA51 and AER-SDNS.

### 4.1 Models

The structured volume mesh used for the AER-NS and AER-SDNS Euler calculations has around 0.8 million cells. Its surface discretization is shown in Figure 5. The small disturbance aerodynamics have been computed for Mach 0.2 to 1.2 and for reduced frequencies based on its reference chord between 0.01 and 3.6. 20 structural modes have been considered, including the 6 rigid-body modes (translations in flow, lateral and vertical directions, roll, pitch and yaw).

The angle of attack of the reference steady solution of AER-NS is computed at an angle of attack of  $0^\circ$ . The configuration has some wing-twist inducing nonzero overall forces and moments.

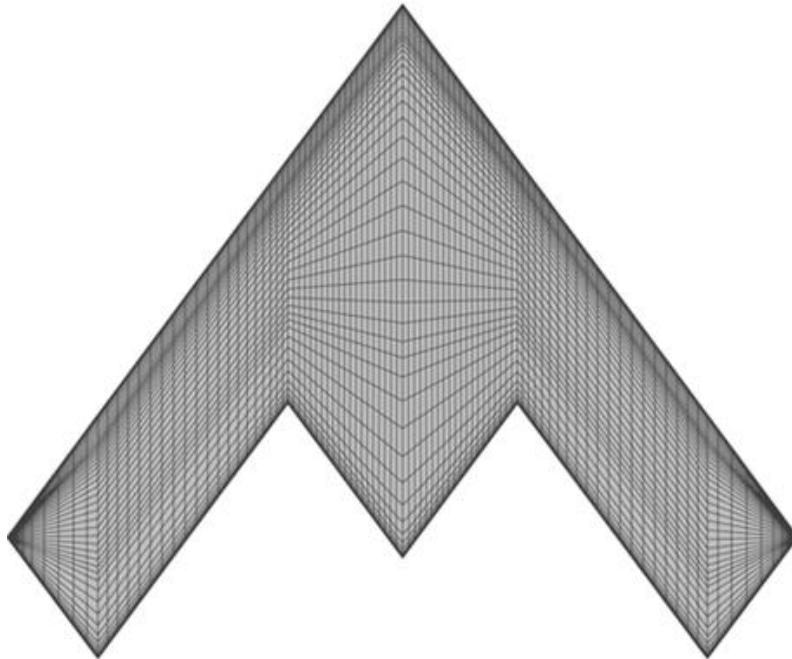


Figure 5: CFD Euler surface mesh

The DLM/ZONA51 mesh with 240 boxes used in this paper is presented in Figure 6 and is coarser than the one used in [9]. However, the accuracy of the results is not affected.

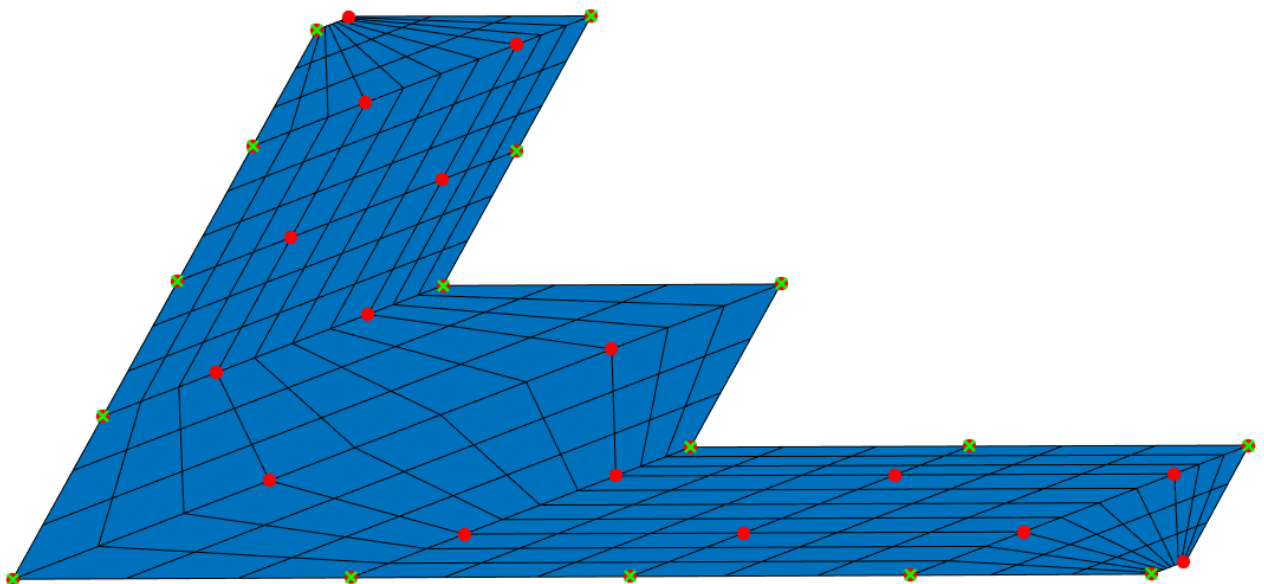


Figure 6: DLM/ZONA51 mesh, with reference points for forces (red) and downwash smoothing (green crosses)

The additional reference points plotted in Figure 6 will be discussed in the following section.

## 4.2 Aerodynamic correction method and results

The present correction method is used for the whole Mach and reduced frequency ranges, considering three rigid-body modes for its training, namely the heave (3), roll (4) and pitch (5) modes for the AIC-correction part. Because of the specifics of this flying wing configuration, no improvement can be expected from the other rigid-body modes aerodynamics, since these ones cannot produce any downwash in the case of DLM/ZONA51.

A first run of the AIC-correction delivered a perfect match for the training modes GAFs. However, the correction of the downwash was not very smooth, raising concerns that the correction may be too specific to the only training modes. Thus, smoothing techniques have been applied.

On the side of the aerodynamic forces, the AIC-correction methods bases on an equality of forces, usually at each box of the DLM/ZONA51 mesh. Using an additional IPS-spline [10], this equality of forces condition has then only to be fulfilled at the reference points for forces shown in Figure 6. One should note that this has no effect on the overall forces and moments of the aerodynamics of the training modes.

A second smoothing technique is used on the downwash side. Instead of inverting the AIC matrix in order to obtain the equivalent downwash of AER-SDNS out of the pressure forces, a least-square technique is used in order to minimize the difference of the forces between DLM/ZONA51 and AER-SDNS. The difference in angle of attack must follow an IPS-spline surface based on the reference points for downwash presented in Figure 6. The resulting smoothed downwash inputs from AER-SDNS for the AIC-correction part are presented in Figure 7 in the case of the pitching mode at Mach 0.6 and reduced frequency 0.01. The color scale for both pictures gets from 0.25 (blue) to 0.7 (yellow), whereas the pitch angle of the mode was set to 0.5 (as in the DLM case).

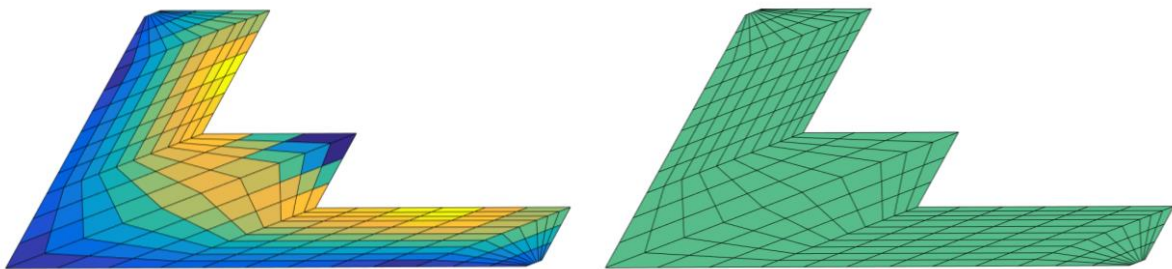


Figure 7: downwash (real part) at Mach=0.6 and  $k=0.01$  for AER-SDNS (left) and DLM (right)

The resulting smoothed forces of AER-SDNS splined in the DLM mesh can be compared with the non-corrected DLM forces in Figure 8, also for the pitch mode.

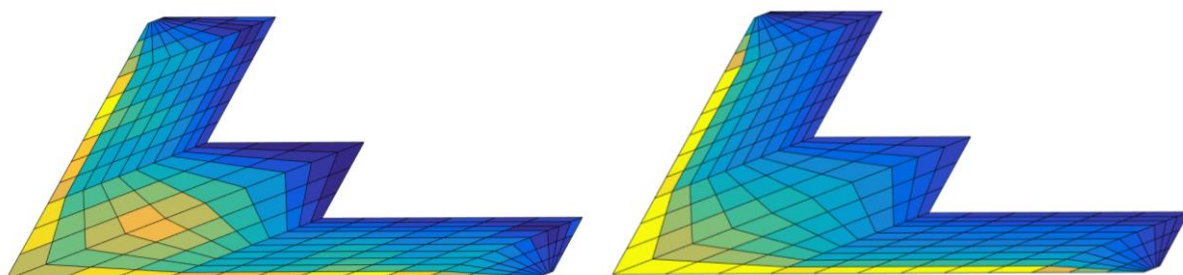


Figure 8: pressure forces (real part) at Mach=0.6 and  $k=0.01$  for AER-SDNS (left) and DLM (right)

The resulting AIC-correction is well-behaved as can be seen in Figure 9.

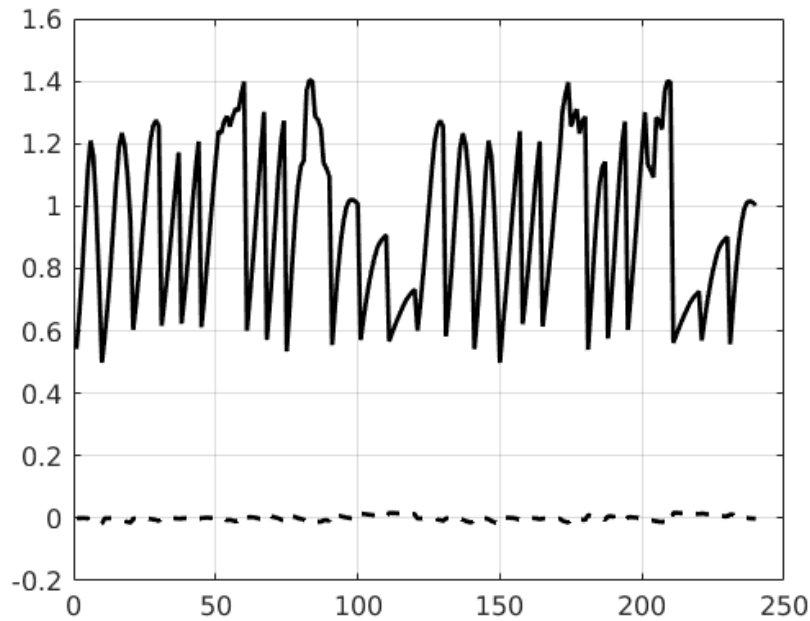


Figure 9: diagonal of the downwash correction matrix at Mach=0.6 and  $k=0.01$

In Figure 9, the real part (full line) of the diagonal of the downwash correction shows a smooth and typical behavior, where the downwash of the leading and trailing edge boxes of the DLM mesh get reduced whereas the boxes in-between see their downwash increased. The imaginary part that would be a correction for phase delay between DLM and AER-SDNS is very low, as a result of very similar frequency trends between both methods. Some corrected GAFs at Mach 0.6 are presented in Figure 10.

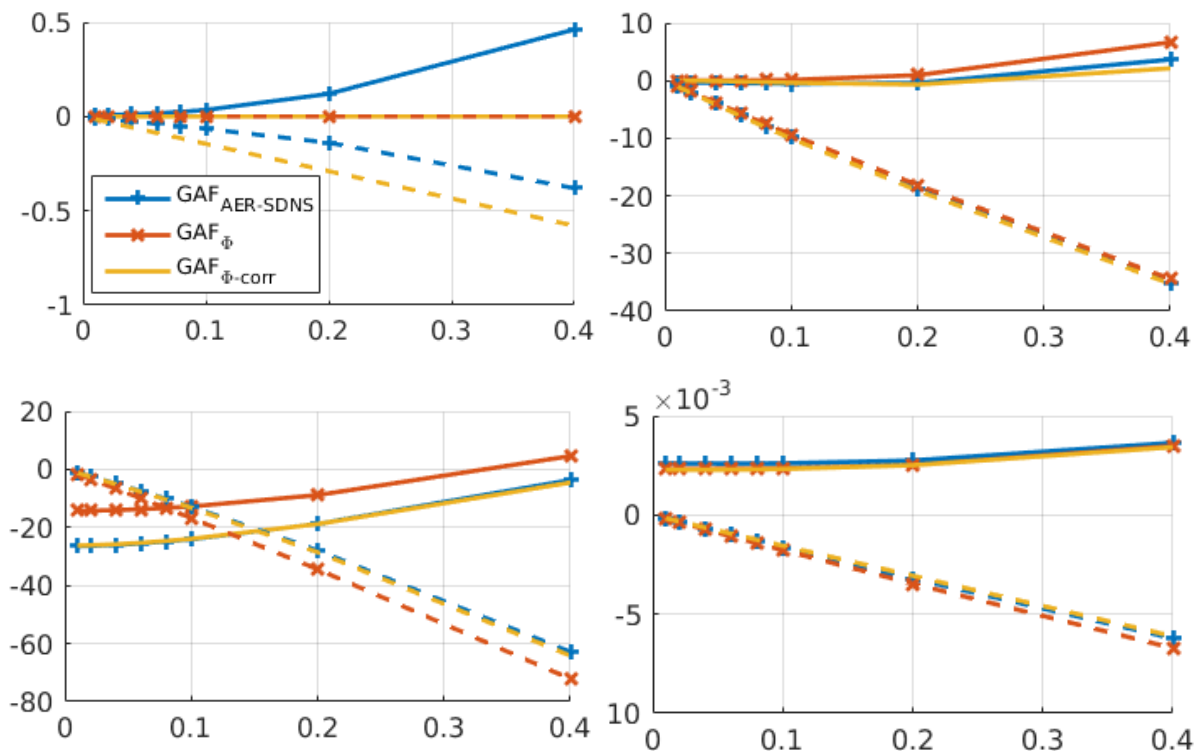


Figure 10:  $GAF_{11}$  (top left),  $GAF_{33}$  (top right),  $GAF_{55}$  (bottom left) and  $GAF_{77}$  (bottom right) at Mach 0.6



In Figure 10, the quality of the GAF-correction can be assessed at Mach 0.6 for some diagonal terms of the GAF matrices for reduced frequencies from 0.01 to 0.4. The yellow curves of the corrected GAFs match very well the blue ones of AER-SDNS even when the DLM ones in red differ, this as well for the training modes 3 (heave) and 5 (pitch) as for the first symmetric bending mode (7). The chord-wise translation mode (1) also gets improved GAFs through the dynamic pressure correction of DLM.

### 4.3 Flutter results

The promising aerodynamic improvements are assessed in this section with respect to flutter stability for the whole Mach and altitude range of the SACCON configuration. For this end, three flutter crossings already identified in [9] are used:

- A symmetric body-freedom flutter mode (coupling heave, pitch and first symmetric bending and torsion modes), in the following called BFF
- An antisymmetric bending-torsion flutter mode (coupling the first antisymmetric wing bending and torsion modes), in the following called Anti
- A symmetric (mostly) in-plane bending-torsion flutter mode (involving the first mostly in-plane wing bending and the first wing torsion), in the following called IP

In [9] one can observe already similar flutter predictions for the first two flutter modes, however, the IP flutter mode is predicted to be strongly more critical by CFD.

The fixed Mach and density flutter analyses of this paper are done using IDEA, an in-house implementation of the PK-method. All the results are presented in term of Mach-altitude-equivalent air speed (EAS) or frequency surfaces in the following subsections.

#### 4.3.1 BFF mode

In Figure 11, the flutter envelopes of the BFF mode are shown. It has to be noted that the flutter mode shape was not strongly affected by the chosen aerodynamic method.

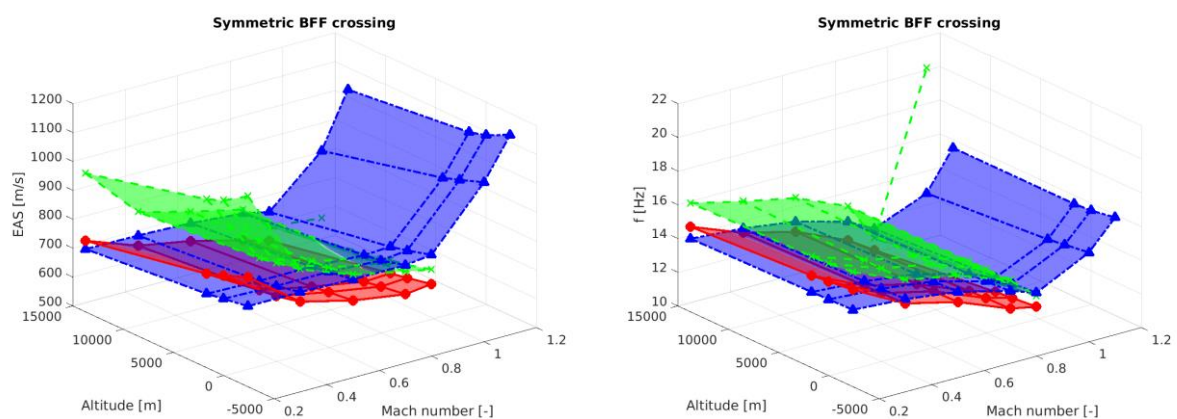


Figure 11: flutter envelopes of the BFF mode

The DLM/ZONA51 non-corrected results are plotted in blue in Figure 11. The match between AER-SDNS (red) and the corrected DLM/ZONA51 (green) is good, showing very similar trends over the Mach and altitude range. Both suffer at Mach 0.2 from the limits of the used CFD-mesh that should be refined in order to avoid the degradation of the AER-SDNS prediction in the incompressible domain. The overall differences about 10% in EAS are acceptable for

such a rapid correction technique. The lack of results in the supersonic domains when using CFD data is due to the fact that the flutter speed was too high for the velocity range set in the flutter analysis.

### 4.3.2 Anti mode

In Figure 12, the flutter envelopes of the Anti mode are shown. Again, it has to be noted that the flutter mode shape was not strongly affected by the chosen aerodynamic method.

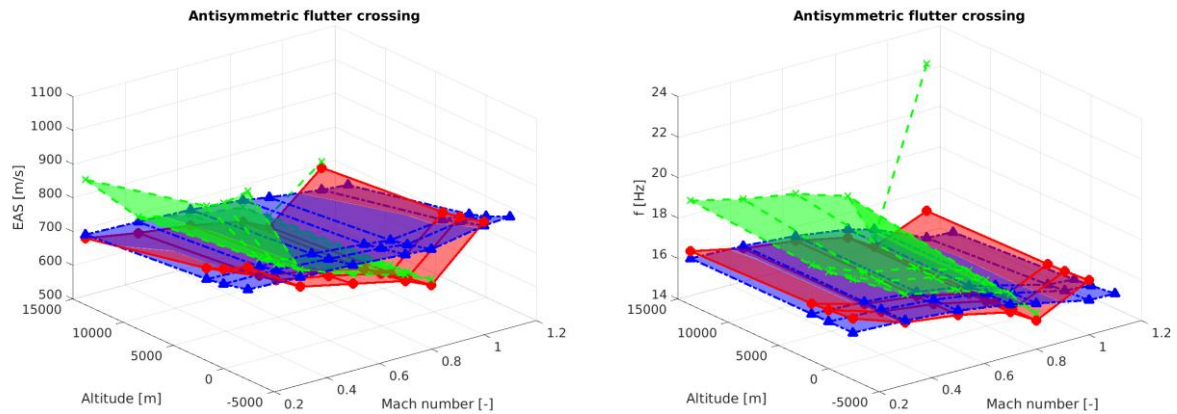


Figure 12: flutter envelopes of the Anti mode

The match between AER-SDNS and the corrected DLM/ZONA51 is similar in quality and precision to the case of BFF.

### 4.3.3 IP mode

In Figure 13, the flutter envelopes of the IP mode are shown. Once again, it has to be noted that the flutter mode shape was still not strongly affected by the chosen aerodynamic method.

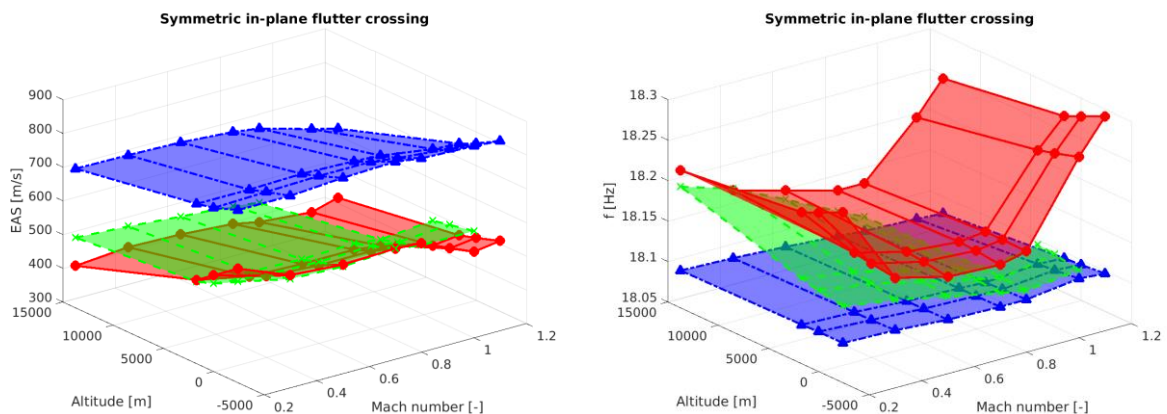


Figure 13: flutter envelopes of the IP mode

The match between AER-SDNS and the corrected DLM/ZONA51 is similar in quality and precision to the case of BFF. However, this time one can appreciate the improvement due to the present correction of DLM/ZONA51 in term in flutter prediction. The predicted flutter speed and frequencies match the AER-SDNS results with high accuracy and cover mostly the original gap between the non-corrected DLM/ZONA51 and AER-SDNS.

#### 4.3.4 Flutter summary and discussion of the results

In Figure 14, the Mach-EAS flutter stability envelopes of the SACCON configuration (considering all altitudes) are shown for all three aerodynamic methods.

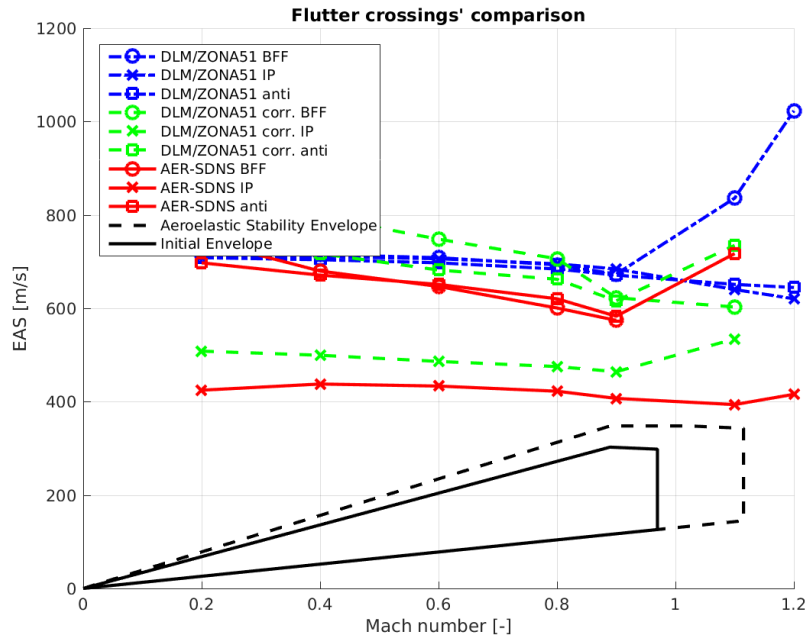


Figure 14: Mach-EAS stability envelopes of the SACCON configuration

Figure 14 shows clearly the gain in prediction accuracy due to the present correction method as well as the precision to be expected in comparison to flutter calculations with the full AER-SDNS dataset. Flutter cases as the IP mode traditionally poorly predicted using the classical DLM/ZONA51 methods can already be assessed using this correction technique.

Considering that only 3 modes out of 20 have to be computed and that, as shown in [5], less Mach numbers and reduced frequencies could be used to train the AIC-correction matrices, one can realistically achieve such an improvement with only 5 to 10% of the computational effort needed for the complete small disturbance CFD dataset, and even less if the modal basis used for flutter predictions is larger.

## 5 CONCLUSIONS

The present correction technique has been developed and tested for the NLR7301 airfoil and the SACCON configuration. The aerodynamics force prediction accuracy can be increased with such a correction.

The added terms in comparison to a pure AIC-correction technique also help increasing the flutter prediction quality of DLM/ZONA51 in the direction of AER-SDNS results.

The additional smoothing features for the forces and downwash make the correction technique more robust for realistic configurations like SACCON.

The strong reduction in term of computational effort allows to introduce first improvement of DLM/ZONA51 aerodynamics very soon in a classical aircraft development process.

## 6 REFERENCES

- [1] E. Kreiselmaier, B. Laschka, “Small Disturbance Euler Equations: Efficient and Accurate Tool for Un-steady Load Prediction”, *Journal of Aircraft*, Vol. 37 No. 5, 2000, pp. 770–778.
- [2] C. Vidy, L. Katzenmeier, M. Winter, C. Breitsamter, ” Verification of the use of small-disturbance CFD aerodynamics in flutter and gust analyses for simple to highly complex configurations”, *International Forum on Aeroelasticity and Structural Dynamics*, 2015, IFASD-2015-066.
- [3] E. Albano, P. Rodden, “A Doublet Lattice method for calculating lift distributions on oscillating surfaces in subsonic flows”, *AIAA paper*, No. 68-73, 1968.
- [4] C. Vidy, L. Katzenmeier, M. Winter, C. Breitsamter, “Efficient and Accurate Aeroelastic Analyses Based on Small-Disturbance CFD in Early Aircraft Development”, *International Forum on Aeroelasticity and Structural Dynamics*, 2017, IFASD-2017-205.
- [5] L. Katzenmeier, C. Vidy, C. Breitsamter, “Correction Technique for Quality Improvement of Doublet Lattice Unsteady Loads by Introducing CFD Small Disturbance Aerodynamics”, *ASD Journal* (2017), Vol. 5, No. 1, pp. 17-40.
- [6] L. H. van Zyl, E. H. Mathews, “Aeroelastic Analysis of T-Tails Using an Enhanced Doublet Lattice Method”, *Journal of Aircraft*, Vol. 48, No. 3, May–June 2011.
- [7] R. J. Zwaan, “Summary of Data Required for the AGARD SMP Activity ‘Standard Aeroelastic Configurations’ – Two-Dimensional Configurations”, *NLR*, MP 79015 U, 1979.
- [8] A. Voss and T. Klimmek, "Design and sizing of a parametric structural model for a UCAV configuration for loads and aeroelastic analysis," in *Deutscher Luft- und Raumfahrtkongress*, 2015.
- [9] D. Schaefer, C. Vidy, C. Mack, J. Arnold, “Assessment of Body-Freedom Flutter for an Unmanned Aerial Vehicle”, in *Deutscher Luft- und Raumfahrtkongress*, 2017.
- [10] W. Rodden and E. Johnson, "MSC/NASTRAN Aeroelastic Analysis User's Guide", MSC, 1994.

## COPYRIGHT STATEMENT

The authors confirm that they, and/or their company or organization, hold copyright on all of the original material included in this paper. The authors also confirm that they have obtained permission, from the copyright holder of any third party material included in this paper, to publish it as part of their paper. The authors confirm that they give permission, or have obtained permission from the copyright holder of this paper, for the publication and distribution of this paper as part of the IFASD-2019 proceedings or as individual off-prints from the proceedings.